Enhanced interfacial interaction, mechanical properties and thermal stability of basalt fiber/epoxy composites with multi-scale reinforcements

Dong Xiang[1, 6, 7, *, #], Tao Shui[1,#], Hongjuan Qiao[2], Wei Tan[3], Eileen Harkin-Jones[4], Jie Zhang[5], Peizhi Ji[2], Ping Wang[1, 6, 7], Bin Wang[1, 6, 7], Chunxia Zhao[1, 6, 7], Hui Li[1, 6, 7], Yuanpeng Wu[1, 6, 7,*] , Yuntao Li[1, 6, 7,*]

[1]School of New Energy and Materials, Southwest Petroleum University, Chengdu 610500, China

[2]Sichuan Aerospace Changzheng Equipment Manufacturing Co., Ltd., Chengdu 610100, China

[3]School of Engineering and Materials Science, Queen Mary University London, London, UK, E1 4NS, United Kingdom

[4]School of Engineering, Ulster University, Jordanstown BT37 0QB, UK

[5]School of Mechanical Engineering, Southwest Petroleum University, Chengdu 610500, China

[6]The Center of Functional Materials for Working Fluids of Oil and Gas Field, Sichuan Engineering Technology Research Center of Basalt Fiber Composites Development and Application, Southwest Petroleum University, Chengdu 610500, China

[7]Collaborative Scientific Innovation Platform of Universities in Sichuan for Basalt Fiber, Southwest Petroleum University, Chengdu 610500, China

*Corresponding authors:

dxiang01@hotmail.com (Dong Xiang);

yuntaoli@swpu.edu.cn (Yuntao Li);

ypwu@swpu.edu.cn (Yuanpeng Wu)

[#]These authors contributed equally to this work.

Abstract

In this work, epoxy (EP) resin composites with multis-cale reinforcements were prepared by hand lay-up and hot-pressing. The epoxy was reinforced with basalt fibers (BF) modified with a silane coupling agent (KH560). Carboxylated multi-walled carbon nanotubes (CNTs) were also grafted onto the surface of the modified BF using an impregnation method to achieve BF/CNTs multi-scale reinforcement. Fourier transform infrared spectroscopy (FTIR) and X-ray photoelectron spectroscopy (XPS) showed that KH560 was successfully grafted onto the BF surface. Scanning electron microscopy (SEM), indicated a better resin adhesion on the BF and thus a stronger interfacial interaction in the BF/CNTs-reinforced composite. It was observed that the mass fraction of KH560 was a significant parameter in achieving desirable CNT immobilization and mechanical properties of the composites. At an optimal mass fraction of KH560 (5%), the tensile, flexural, and interlaminar shear strength (ILSS) of the modified composite (BF-5%KH560-CNT/EP) increased by 12.5%, 20.9%, and 25.5% respectively

compared with the BF-washed/EP composite due to more efficient load transfer. In addition, compared with BF-washed/EP, the decomposition onset temperature of BF-5%KH560-CNT/EP increased from 387 ℃ to 396 ℃, the maximum decomposition rate temperature increased from 400 ℃ to 408 ℃, and the residual weight increased by 5.8%.

Keywords: Basalt fiber, Composite, Interface, Mechanical properties, Thermal stability

1. Introduction

Basalt fiber (BF) is a high-performance fiber material made from melting of volcanic rock. Its chemical composition and structure are similar to glass fiber [1-3] and it has excellent mechanical, chemical, thermal, and weather resistance properties [2,4,5]. At present, BF has been used in fields from aerospace to automobile and from building construction to energy conservation[6-12].

Fiber-reinforced polymer (FRP) composites have the advantages of lightweight, low cost, corrosion resistance and high performance, and are gradually replacing traditional structural (metal or inorganic) materials in some fields [13]. The application of FRP composites in fields such as civil engineering, transportation, aerospace, and other fields is also increasing [6,14,15]. The properties of these composites are mainly determined by the material properties of reinforcements and matrix and their respective volume fractions, as well as the properties of the interface layer. As the third phase, the interfacial phase has physical and chemical properties which affect

how the load is transferred from the "weak" matrix to the "strong" fiber, and from one fiber to the next through the matrix [16]. The load transfer capacity of the interfacial phase depends largely on the adhesion between fiber and matrix [17]. Because the surface of BF is very smooth and chemically inert, the interfacial adhesion between the BF and resin matrix is poor, which limits its application in composite materials [18-20]. To improve the interfacial interaction, surface modification of BF is carried out by treating the fiber surface using chemical or physical methods, or by coating nanomaterials on the fiber surface. In the past decade or so, a lot of work has been carried out on the surface modification of basalt fiber to improve its interface performance by methods such as plasma modification, oxidation modification, coating modification, and multi-scale reinforcement based on nanomaterials[21-30].

Among the BF surface modification methods mentioned above, the use of multi-scale reinforcements has attracted much attention due to its excellent modification effect, designability, and excellent interface properties[28,31-33]. Differing from other surface modification methods, multi-scale reinforcement attaches a secondary nano-scale reinforcement on the BF surface to form a transition zone to transfer load and reduce stress concentration[16]. In recent years, a small number of studies have focused on multi-scale reinforced materials to improve the mechanical properties of BF reinforced polymer composites. For example, Hou et al.[34] assembled SiO_2 nanoparticles on the surface of short BF using a hydrothermal method, and improved the interface interaction between polylactic acid (PLA) and BF with silane coupling agent KH550. Their experimental results showed that the tensile

strength and flexural strength of PLA/BF composites increased by 18.40% and 15.28% respectively with the introduction of SiO_2 on the surface of BF. Nicoleta et al.[10] deposited ZnO nanoparticles on the surface of BF by chemical deposition, which increased the interfacial shear strength (IFSS) by 42%. He et al.[35] modified the BF surface with a mixed solution of polycaprolactone (PCL) and SiO_2 nanoparticles, which increased the tensile strength of the PLA/BF composite by 29%. Mittal et al.[36] used chemical vapor deposition (CVD) to graft CNTs onto BF fabrics. The results showed that the volume conductivity and electromagnetic interference (EMI) shielding effect of BF/CNTs reinforced epoxy resin composites were improved by attaching CNTs on the BF surface. Although studies have been conducted on nanoparticle addition on the BF surface, most of these studies focus on one particular mechanical property of the basalt fiber reinforced composite. In addition, the preparation of multi-scale reinforcing materials usually includes multiple, complex and time-consuming processes[37], which limits the adoption of these composite materials for mass-scale industrial production. Moreover, some modification methods have been shown to damage the surface of the BF to some extent, resulting in a reduction of mechanical properties of the BF[32,38]. It is, therefore, very important to develop a rapid and effective preparation method for multi-scale reinforcing materials without sacrificing the mechanical properties of the fibers.

BF has good thermal stability and BF-reinforced polymer composites therefore have good potential in high-temperature resistance applications. Garima et al.[39] successfully deposited graphene oxide on the surface of BF by electrophoretic

deposition, and then reduced the graphene oxide to delay the crystallization of BF from 697 ℃ to 716 ℃. This confirmed that graphene coating plays a protective role in the high-temperature crystallization of BF. However, there is very limited literature focusing on the influence of BF surface modification on the thermal properties of its composites to date.

In this work, multi-scale BF/CNT reinforcement was prepared in two steps. In the first step, pristine BF was treated with KH560 to make it serve as a bridge between the BF and carboxylated CNTs which were grafted on the surface of the BF in a second step. Multi-scale BF/CNT reinforced epoxy composites were prepared by hand lay-up and hot-pressing. The influence of KH560 mass fraction on the immobilization of carbon nanotubes and the interfacial properties of the composites was investigated. The interface strengthening mechanism of the composite was discussed in detail in this paper. To the best of the author's knowledge, the effect of silane coupling agent KH560 and carboxylated CNTs on the mechanical properties of BF has not been reported earlier. The composite preparation method presented in this work has the advantages of short processing time, simple operation, and no damage to the BF. This is of great significance in helping to further promote the application of basalt fiber composites.

2. Experimental

2.1Materials

Continuous basalt fiber (BC9-180) with an average diameter of 9 μm was

purchased from Sichuan Aerospace Tuoxin basalt Industrial co., LTD. 3-glycidyl ether oxy-propyl tri-methoxy silane (KH560) was purchased from Jinan XingFeiLong Chemical co., LTD., China. Carboxylated multi-walled carbon nanotubes (CNTs) (inner diameter 5-10 nm, outer diameter 8-15 nm, length 5-15 μm) (>98%) were purchased from Shenzhen SuiHeng Technology co., LTD., China. Acetone, ethanol, and acetic acid were purchased from Chengdu Kelong Chemical Reagent Factory. Epoxy resin (WSR618 E51) was purchased from Nantong Xingchen synthetic materials Co., LTD. The curing agent, methyl tetrahydro phthalic anhydride, was purchased from Jiulimei Electronic Materials Co., LTD. China.

2.2 Surface modification of basalt fiber

The BF was cut into 18 cm long sections, and then heated with acetone in an oil bath at 60 ℃ for 8 h to desize. After taking the BF out of the oil bath, it was cleaned by deionized water and dried. A mixture of ethanol and deionized water was prepared according to a mass ratio of 95:5. KH560 with different mass fractions (1%, 3%, 5%, 10%) was added to it and this was treated with an ultrasonicator for 1 h. To promote a hydrolysis reaction of KH560, some acetic acid was added to the mixed solution to adjust its pH value to 5. The hydrolysis reaction of KH560 is shown in Fig. 1 (a). The desized BF was added into a KH560/ethanol/deionized water solution and kept for 12 h at 50 ℃. After taking the treated BF out, it was washed with ethanol, then allowed to dry. The resulting basalt fibers are denoted as BF-X% KH560, where X represents the mass fraction of KH560 used for the treatment (X = 1, 3, 5 and 10).

Carboxylated multi-walled carbon nanotubes were put into ethanol, and

ultrasonically treated for 2 h to prepare a suspension with a mass fraction of 0.5%. The prepared BF-X%KH560 fibers were immersed in the CNTs/ethanol suspension for 10 min to allow the CNTs to adsorb on the BF surface. The fibers were then taken out of the suspension and dried in an oven at 50 ℃ for 4 h. The dried basalt fibers are denoted as BF-X% KH560-CNT. The process diagram for the BF surface modification is shown in Fig. 1 (b).

The grafting reaction of BF, KH560 and CNT is shown in Fig. 1 (c). There are two main mechanisms of chemical grafting of the basalt fiber and silane coupling agent[33,40,41]. In the first, the silanol generated by hydrolysis of the silane coupling agent KH560 underwent an etherification reaction with the hydroxyl group on the surface of the basalt fiber to generate Si-O-Si. The etherification reaction also took place between silanols. In the second mechanism, the KH560 hydrolyzed silanol generated hydrogen bonds with hydroxyl group on the surface of the basalt fiber and between silanol molecules. The surface of the basalt fiber grafted with KH560 became rough with attachments and small protrusions, which provided favorable conditions for CNT adhesion. In addition, the carboxylated CNTs reacted with the grafted KH560 on the BF surface to form chemical bonds, which made CNTs graft onto the BF surface.

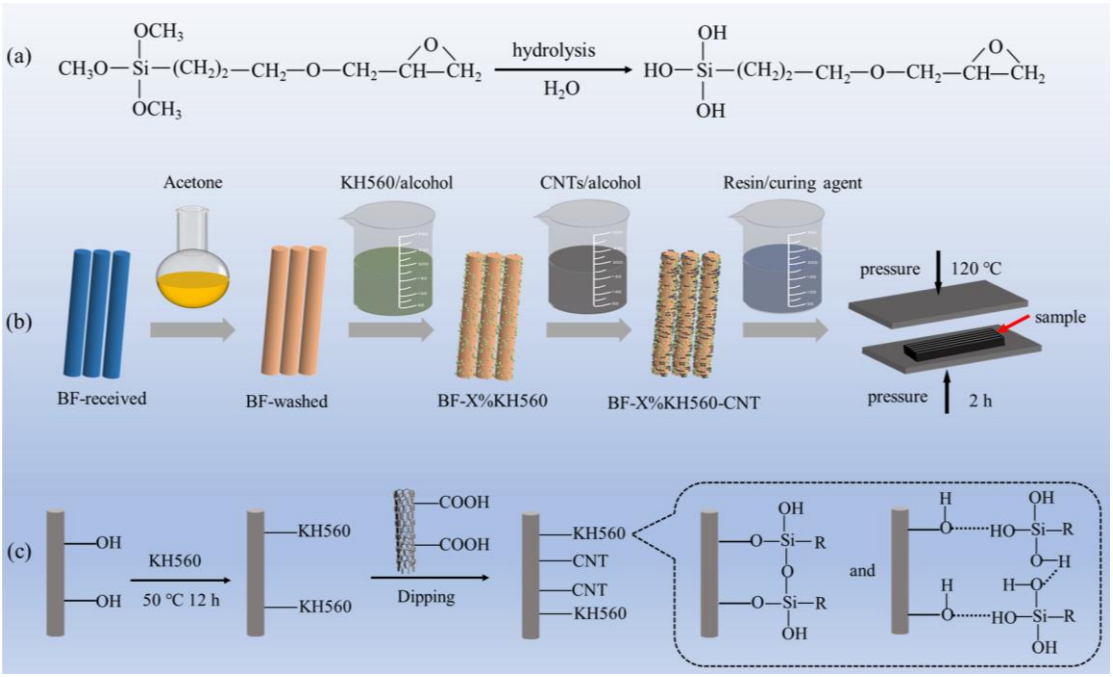

Fig. 1 (a) KH560 hydrolysis reaction formula, (b) Schematic diagram of BF modification and composite material preparation, (c) Schematic diagram of BF grafted with KH560 and CNTs

2.3 Preparation of basalt fiber epoxy composite

To prepare the basalt fiber epoxy composite, epoxy resin and curing agent were first mixed in a mass ratio of 10:8 and stirred evenly. Then BF-X%KH560 and BF-X%KH560-CNT were manually impregnated by the epoxy resin and curing agent. The impregnated basalt fibers were laid unidirectionally in a mold, and then cured at 10 MPa and 120 ℃ for 3 h in a hot-pressing machine to prepare BF/KH560 and BF/KH560/CNT reinforced epoxy matrix composites (Fig. 1 (b)). The resulting composite materials are denoted as BF-X%KH560/EP and BF-X%KH560-CNT/EP.

2.4 Characterization

The surface chemical properties of the basalt fibers were examined using Fourier

transform infrared spectroscopy (FTIR, Thermo Scientific Nicolet 6700, USA) and X-ray photoelectron spectroscopy (XPS, Thermo Scientific Nexsa, UK) techniques. The surface morphology of basalt fibers before and after modification and fracture surface of composites were observed by scanning electron microscopy at 20 kV after being sprayed with gold (SEM, ZEISS EV0 MA15, Germany).

Mechanical testing of the developed composite samples included tensile, flexural (3-point bending), and interlaminar shear strength (ILSS) tests. Five specimens were used for each test, and the average value was taken. Tensile testing was carried out on standard tensile specimens cut from the hot-pressed basalt fiber composite sheets according to GB/T 1447-2005. The test was carried out on an electronic, universal material testing machine (AG-50KNXPLUS) equipped with a 50 kN load cell at a quasi-static loading rate of 2 mm/min at room temperature. For the flexural test, standard three-point bending test specimens were cut from the hot-pressed composite sheets according to GB/T 1449-2005. The size of the specimen was 40 mm × 15 mm × 2 mm and the span thickness ratio was 16:1. The flexural test was carried out at room temperature on a universal material testing machine (CMT4104) equipped with a 10 kN load cell at a quasi-static loading rate of 2 mm/min. ILSS testing was performed according to GB/T 30969-2014 on standard shear specimens cut from the hot-pressed basalt fiber composite laminates. The size of the interlaminar shear specimen was 20 mm × 6 mm × 2 mm. This test was also carried out at room temperature using the CMT4104 universal material testing machine at a quasi-static loading rate of 2 mm/min.

Thermogravimetric analysis (TGA) was carried out on the composites using a thermal analyzer (DSC823TGA/SDTA85/e) in a nitrogen (20 ml/min) atmosphere, from room temperature to 800 ℃, with a heating rate of 20 ℃/min.

3. Results and discussion

3.1 Surface modification and morphology

The chemical functional groups on the surface of BF-washed carboxylated multi-walled carbon nanotubes (MWCNT-COOH), BF-5%KH560, BF-10%KH560, BF-5%KH560-CNT, BF-10%KH560-CNT were analyzed using FTIR. The results of the FTIR analysis are shown in Fig. 2. BF-washed, MWCNT-COOH, BF-X%KH560, and BF-X%KH560-CNT all have peaks at ~3445 cm^{-1} and ~1635 cm^{-1}, which is attributed to the stretching and bending vibration of -OH. The peaks at ~2917 cm^{-1} and ~2848 cm^{-1} are due to the anti-symmetric and symmetric stretching vibration peaks of -C-H. All BF peaks at ~860 cm^{-1} and ~470 cm^{-1} are due to Si-O-Si. The C=O vibrational absorption peak of the carboxyl group in the carbon nanotube is located at ~1710 cm^{-1}, and the vibrational peak of the C=C conjugated double bond in the carbon nanotube is located at ~1600 cm^{-1}. The peaks for BF-5%KH560 and BF-10%KH560 at ~1310 cm^{-1} and ~1345 cm^{-1} can be attributed to the stretching vibration peak of the epoxy ring, which indicates that the KH560 is successfully grafted onto the BF. In addition, for the BF-5%KH560-CNT and BF-10%KH560-CNT, the peak value appears at ~1050 cm^{-1}, which is due to the reaction between carboxylated CNTs and KH560 grafted on the surface of BF to

produce Si-O-C[42].

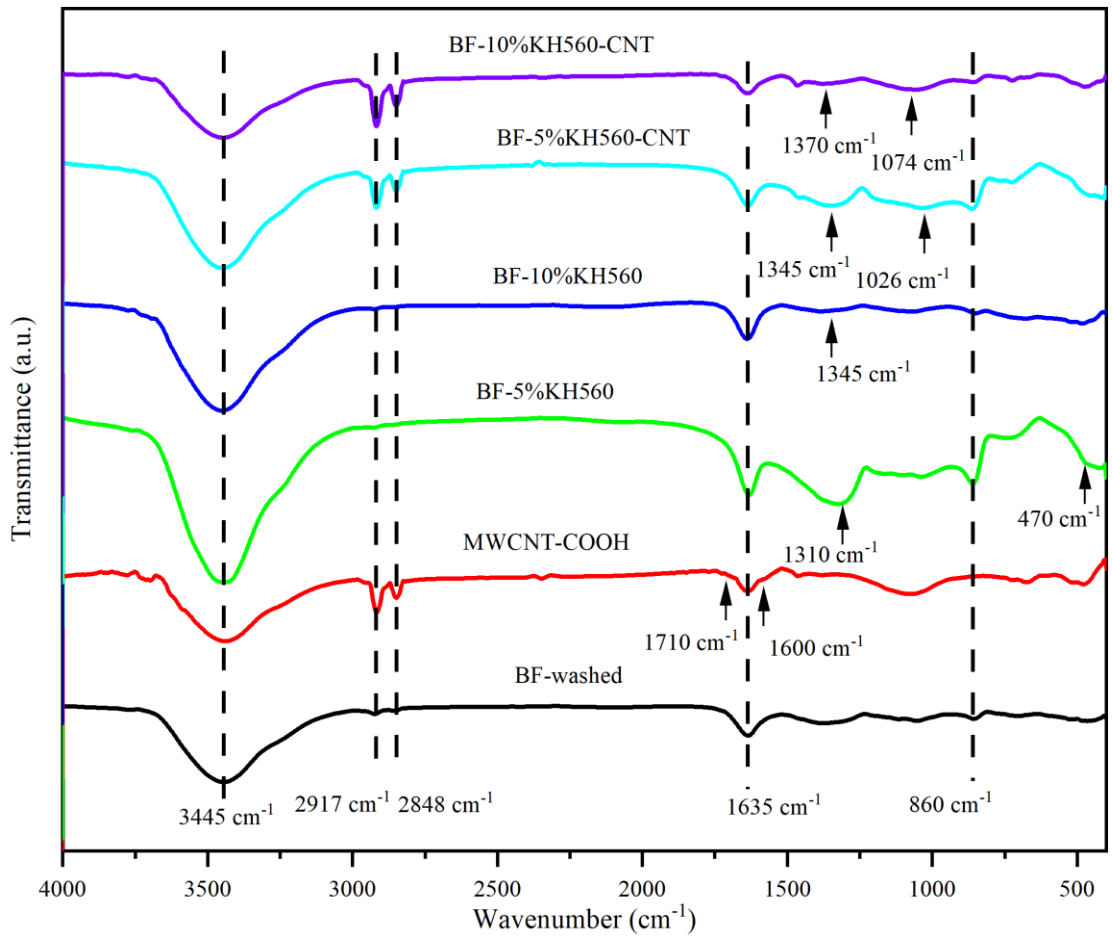

Fig. 2 FTIR spectra of BF-washed, CNT, BF-5%KH560, BF-10%KH560, BF-5%KH560-CNT, BF-10%KH560-CNT

The elemental composition of BF-washed and BF-X%KH560 surfaces was examined using XPS, results shown in Table 1 and Fig. 3. As shown in Table 1, the highest proportion of C appears on the untreated BF. On the other hand, the highest content of O and Si are present on the surface of the BF grafted with KH560.

XPS analysis further confirmed the changes in the BF surface chemical composition due to grafting and the existence of introduced molecular chains after the grafting reaction. The total XPS spectra, C1s spectra, and Si2p spectra of three samples: BF-washed, BF-5%KH560, and BF-10%KH560 are shown in Fig. 3. The

total XPS spectra of the three samples, shown in Fig. 3 (a1), (b1), and (c1) exhibit the characteristic peaks of C1s, O1s, and Si2p. For the BF-washed sample, O1s and Si2p peaks are related to the main chemical components of BF. A possible reason of the C1s peak may be the presence of carbon pollution in the test environment. This has also been reported in other relevant publications[43-46]. As shown in Fig. 3 (a2), (b2), and (c2), compared with the BF-washed material, the C1s spectrum of the BF treated with KH560 shows C-Si at 284.2 eV, and C-O-C at 286.2 eV[28,44,47]. Both of these are from the silane coupling agent KH560, which proves that KH560 is successfully grafted onto the BF. To further confirm the reaction between the BF surface and KH560 molecules and between the KH560 molecules, the Si2p peaks of the BF-washed BF-5%KH560, and BF-10%KH560 were also fitted, as shown in Fig. 3 (a3), (b3), and (c3). It can be seen that Si2p can be fitted to three peaks of 101.87 eV, 102.45 eV, and 103.03 eV, which are respectively attributed to Si-OH, Si-O-Si, and SiO2[46,48]. Table 2 lists the proportions of these three peaks. It can be seen from the data presented in Table 2 that among the silicon chemical bonds on the surface of the unmodified BF, SiO2 accounts for 31.3%, Si-OH accounts for 26.5%, and Si-O-Si accounts for 42.2%. When the BF was modified, the hydrolysate of KH560 reacted with the hydroxyl group on the BF surface, and KH560 molecules reacted with each other to form Si-O-Si, as shown in Fig. 1 (c). This formed a polysilane coupling agent layer on the BF surface. For the samples tested, it was calculated that with the increase of the mass fraction of KH560, the content of the Si-O-Si functional group increased from 42.2% to 55.9%, indicating that the KH560 was grafted onto the BF

surface, and the interaction between KH560 molecules both increased.

Table 1 Content distribution of C, O, and Si elements on the basalt fiber surface before and after KH560 treatment

Samples	Element content, %		
	C	O	Si
BF-washed	69.0	21.5	9.5
BF-1%KH560	60.4	26.1	13.5
BF-3%KH560	58.5	27.3	14.2
BF-5%KH560	57.4	28.0	14.6
BF-10%KH560	59.8	29.1	11.1

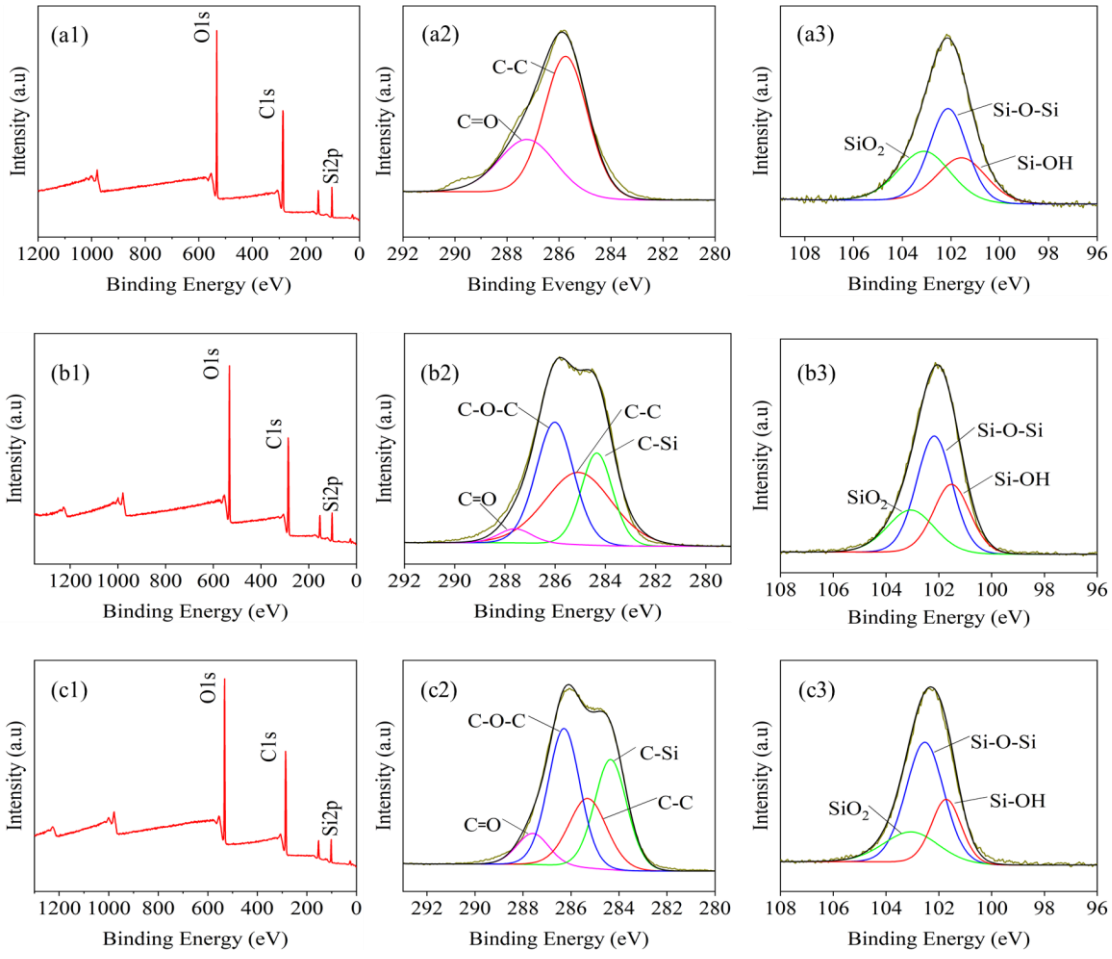

Fig. 3 The XPS spectra of (a) BF-washed, (b) BF-5%KH560 and (c) BF-10%KH560 (1: the total spectrum; 2: the C1s spectrum; 3: the Si2p spectrum)

Table 2 Si2p content of functional groups on the basalt fiber surface before and

after KH560 treatment

Samples	Functional group content, %		
	101.87eV	102.45eV	103.03eV
	Si-OH	Si-O-Si	SiO_2
BF-washed	26.5	42.2	31.3
BF-5%KH560	29.0	48.1	22.9
BF-10%KH560	23.5	55.9	20.6

The surface morphologies of the basalt fiber after desizing and the basalt fiber modified by the silane coupling agent KH560 were examined using a scanning electron microscope. Fig. 4 (a-e) shows the SEM images of the washed basalt fiber without KH560 grafting, BF-1%KH560, BF-3%KH560, BF-5%KH560, and BF-10%KH560 respectively. The SEM images highlight the effect of KH560 in increasing the surface roughness of the BF. In Fig. 4 (a), it can be found that the surface of the BF after desizing is smooth without pores, and there are no obvious grooves or protrusions. A smooth BF surface can lead to poor interfacial adhesion between the BF and resin matrix, which limits its use in composite materials. Fig. 4 (b)-(e) show that the silane coupling agent KH560 increases the surface roughness of the BF, with attachments and small protrusions, which is conducive to improving the mechanical coupling of the BF and epoxy resin matrix. However, when the concentration of silane coupling agent KH560 is increased to 10%, a large amount of silane is physically adsorbed on the fiber surface and this forms a weak interface layer. This reduces the interface adhesion and is not conducive to good composite performance[41,49].

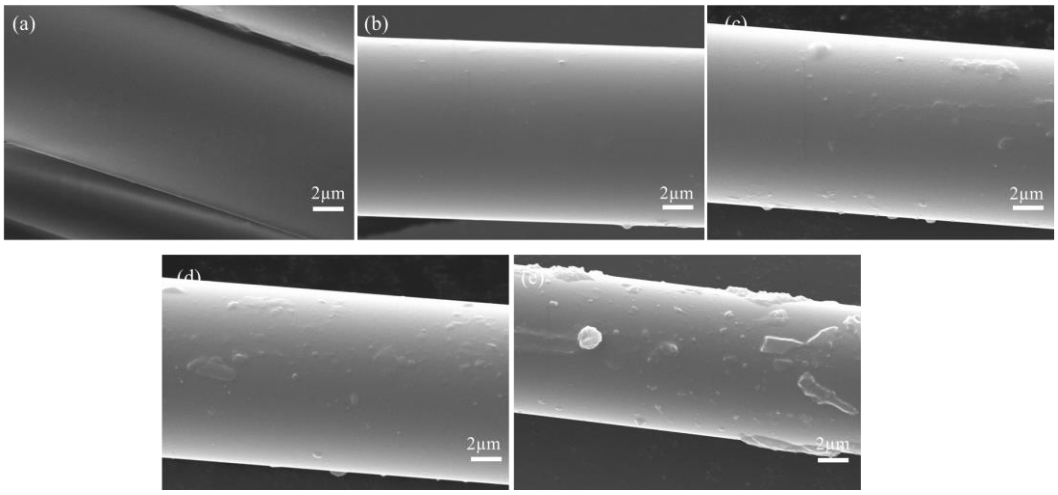

Fig. 4 SEM images of basalt fiber surface before and after KH560 treatment: (a) BF-washed, (b) BF-1%KH560, (c) BF-3%KH560, (d) BF-5%KH560, (e) BF-10%KH560

The surface morphology of the BF-X%KH560 fibers with grafted CNTs was also observed using SEM. The results shown in Fig. 5 highlight that the adsorption of CNTs on the BF surface is strongly affected by the mass fraction of KH560. The adsorption amount increases with the increase in mass fraction of KH560, which indicates that KH560 is an effective coupling agent between the BF and CNTs. It should be noted that when the mass fraction of KH560 is 10%, a large amount of CNTs are adsorbed on the BF surface and become entangled with each other to form aggregates.

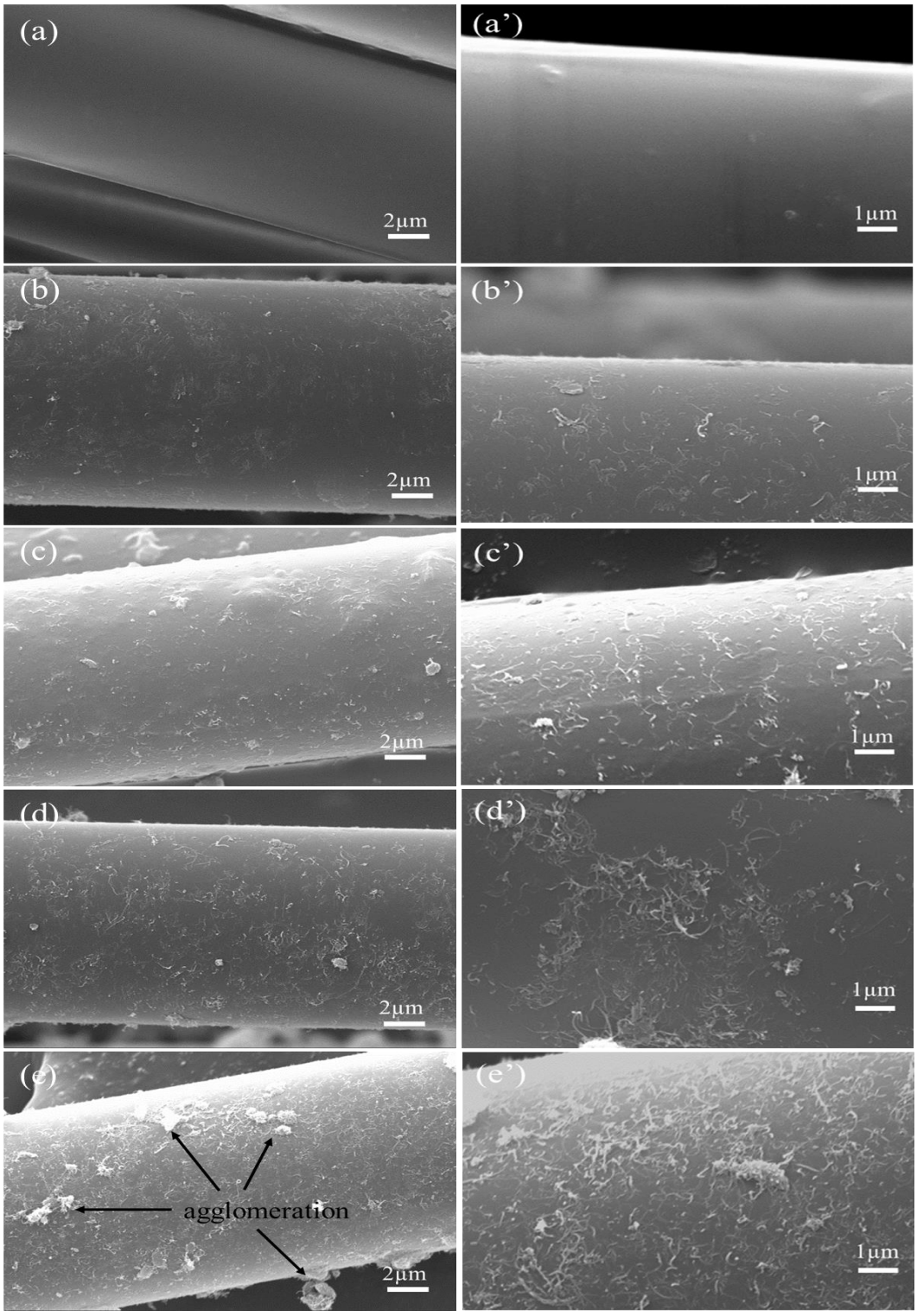

Fig. 5 SEM of BF-X%KH560 surface treated with CNT solution: (a) and (a') BF-washed, (b) and (b') BF-1%KH560-CNT, (c) and (c') BF-3%KH560-CNT, (d) and (d') BF-5%KH560-CNT, and (e) and (e') BF-10%KH560-CNT

3.2 Mechanical properties of composites

3.2.1 Tensile properties

The tensile stress-strain curves of composites are shown in Fig. 6. The tensile modulus, tensile strength, and elongation at break are shown in Fig. 7 and Table 3. It can be seen from that compared with the BF-washed/EP composite, the tensile modulus, tensile strength, and elongation at break of the BF-X%KH560/EP and BF-X%KH560-CNT/EP composites are improved as the mass fraction of KH560 is increased from 0% to 5%. For the BF-X%KH560/EP composites, the best properties were obtained for BF-5%KH560/EP composite for which the tensile modulus, tensile strength, and elongation at break were 42.7 GPa, 599.1 MPa, and 2.7% respectively. This represents an increase of 18.3%, 5.7%, and 15.1% in the three properties respectively, compared to the properties of the BF-washed/EP composite. This improvement can be attributed to the coupling reaction between the silane coupling agent KH560 and the BF. The coupling agent forms a dense protective film on the surface of the BF, which better covers the micro-cracks on the BF surface[50], reduces the impact of microcracks on the tensile properties of the BF, and thus improves the tensile properties of the composite. Besides, the binding force between the BF and epoxy resin matrix after KH560 treatment is enhanced, the interface between the matrix and fiber is improved, and the resistance to external forces is increased[28].

However, the tensile modulus, tensile strength, and elongation at break of the BF-10%KH560/EP were found to be 18.3%, 9.8%, and 12.1% lower than those of the BF-washed/EP. This reduction in properties can be associated with the large amount KH560 which is physically adsorbed on the surface of the BF, forming agglomerates and a weak interface layer with resin.

With the introduction of CNTs to the composites (BF-X%KH560-CNT/EP), a more significant improvement in tensile properties can be observed for the same mass fraction of KH560, as shown in Table 3. One can see that the improvement in mechanical properties of BF-X%KH560-CNT/EP composites is also positively influenced by an increase in mass fraction of KH560 up to 5%. Among the composites tested, the best results were obtained for the BF-5%KH560-CNT/EP, and its tensile modulus, tensile strength, and elongation at break were 46.1 GPa, 637.8 MPa, and 3.2% respectively. This represents an increase of 27.7%, 12.5%, and 38.4% compared with the BF-washed/EP composite. The additional performance improvement compared to the BF-X%KH560/EP composites can be attributed to the carboxylated CNTs which were introduced on the surface of the BF. With the addition of CNTs, the specific surface area and roughness of the fiber are improved, which in turn improves the van der Waals force and mechanical meshing between the fiber and the resin. In addition, the oxygen-containing functional group/unsaturated double bond on the surface of the carboxylated CNTs can react with the epoxy resin matrix to support the chemical connection between the BF and epoxy resin matrix. The resulting interface is stable and strong[33,51,52]. Furthermore, we also conducted impact

tests on the basalt fiber composite materials before and after modification. The results are shown in Table S1 in the supporting information. The results indicate that when X ⩽5, the impact strength of BF-X%KH560/EP and BF-X%KH560-CNT/EP increases with increasing KH560 and CNT contents due to enhanced interfaces and more effective stress transfer.

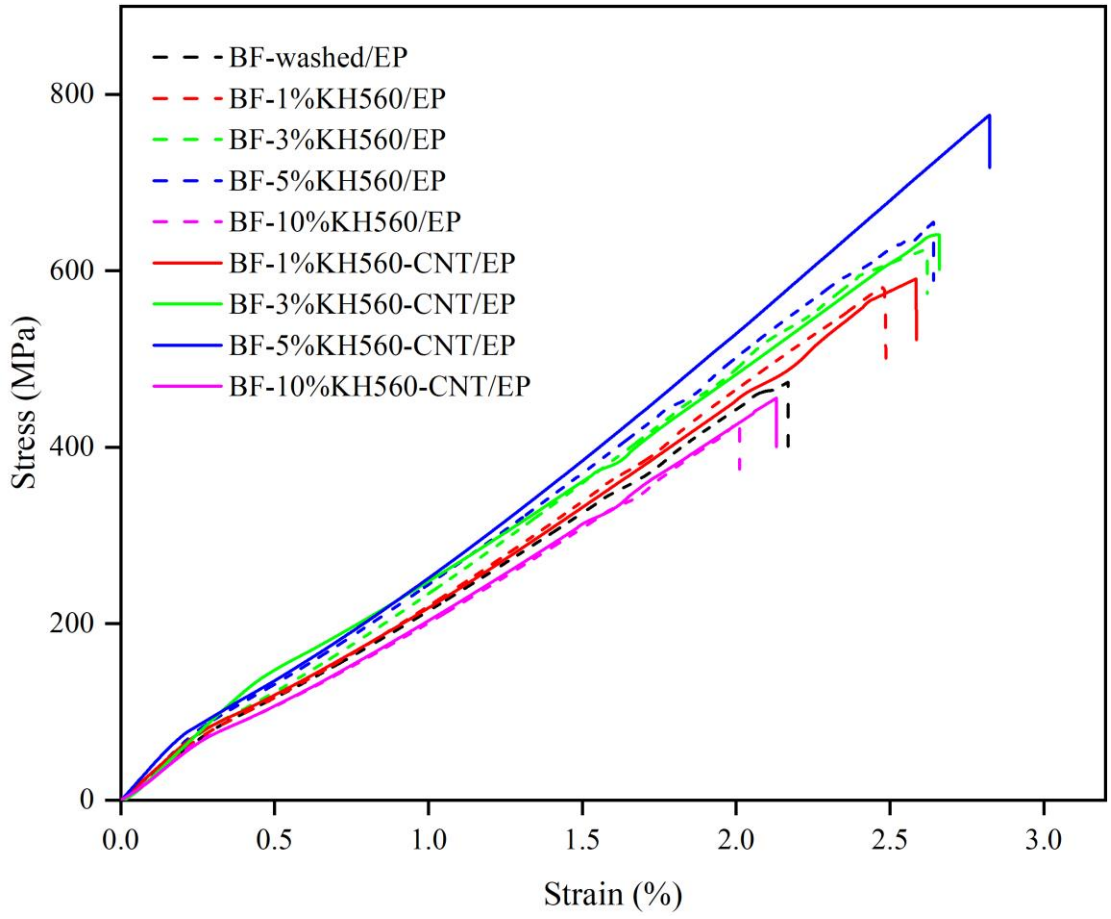

Fig. 6 Tensile stress-strain curves of BF-X%KH560/EP and BF-X%KH560-CNT/EP

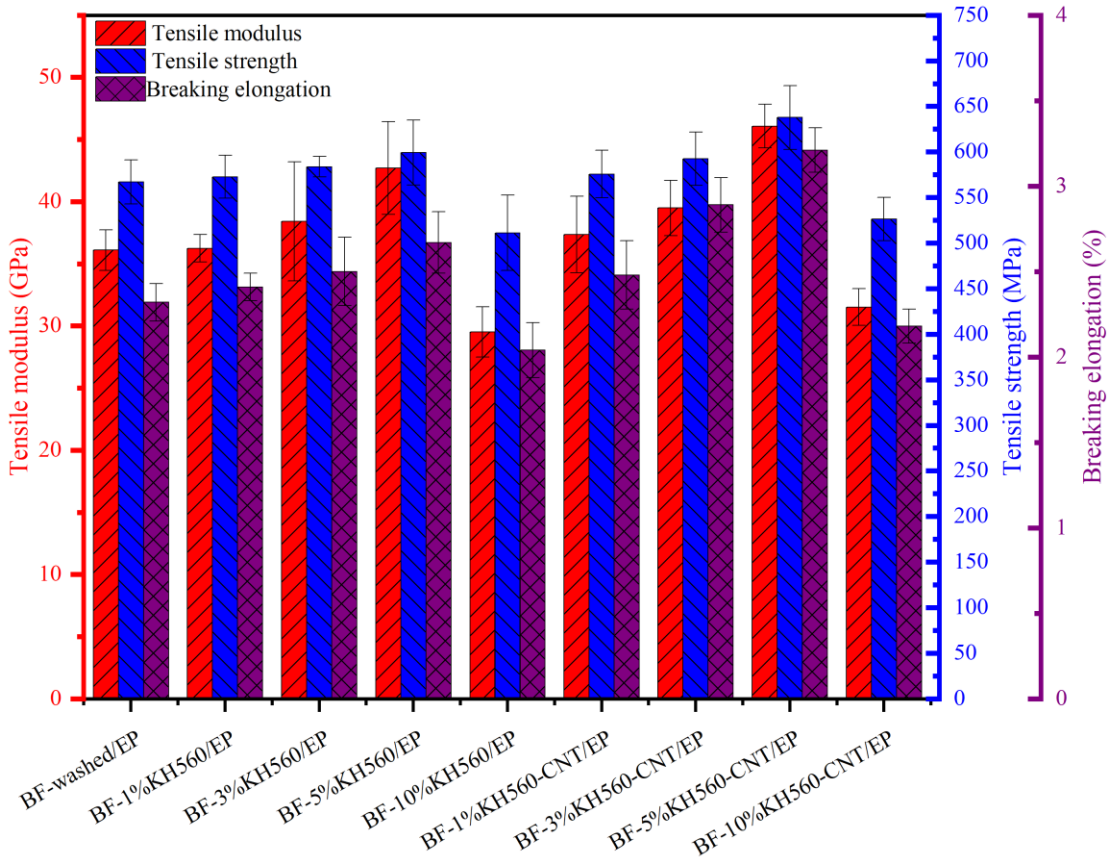

Fig. 7 Tensile modulus (E_t) and tensile strength (σ_t) and elongation at break (ε_t) of modified and unmodified basalt fiber reinforced resin matrix composites

Table 3 Improvement in tensile properties of BF-X%KH560/EP and BF-X%KH560-CNT/EP (standard deviations are shown in the brackets)

Sample	E_t(GPa)	ΔE_t(%)	σ_t(MPa)	$\Delta\sigma_t$(%)	ε_t(%)	$\Delta\varepsilon_t$(%)
BF-washed/EP	36.1(±1.6)	-	566.9(±24.2)	-	2.3(±0.1)	-
BF-1%KH560/EP	36.3(±1.1)	0.6	572.8(±23.7)	1.0	2.4(±0.1)	3.9
BF-3%KH560/EP	38.4(±4.8)	6.4	583.7(±11.1)	3.0	2.5(±0.2)	7.8
BF-5%KH560/EP	42.7(±3.7)	18.3	599.1(±35.6)	5.7	2.7(±0.2)	15.1
BF-10%KH560/EP	29.5(±2.0)	-18.3	511.2(±41.2)	-9.8	2.0(±0.2)	-12.1
BF-1%KH560-CNT/EP	37.4(±3.1)	3.6	575.6(±26.0)	1.5	2.5(±0.2)	6.9
BF-3%KH560-CNT/EP	39.5(±2.2)	9.4	592.4(±29.2)	4.5	2.9(±0.2)	24.6
BF-5%KH560-CNT/EP	46.1(±1.8)	27.7	637.8(±35.1)	12.5	3.2(±0.1)	38.4
BF-10%KH560-CNT/EP	31.5(±1.5)	-12.7	526.4(±23.8)	-7.1	2.2(±0.1)	-6.0

3.2.2 Flexural properties

The flexural stress-strain curves of composites are shown in Fig. 8. The results of flexural testing of the prepared composites are shown in Fig. and Table 4. As shown in the results, for X≤5, the flexural modulus, flexural strength, and flexural strain of BF-X%KH560/EP and BF-X%KH560-CNT/EP are higher than those of the BF washed/EP composite with a larger value of X resulting in better properties. For the same KH560 mass fraction X, BF-X%KH560-CNT/EP composites exhibit better properties than the BF-X%KH560/EP composites, as shown in Table 4. Among the BF-X%KH560/EP composites tested, the best properties were obtained with the BF-5%KH560/EP for which the flexural modulus, flexural strength, and flexural strain are 51.6 GPa, 1332.3 MPa, and 4.0% respectively, an increase of 5.5%, 6.0%, and 12.1% compared with the BF-washed/EP composite. As already discussed in section 3.2.1 on tensile testing, the improvement in properties of the BF-X%KH560/EP composites can be associated with the surface repairing effect of the KH560 which reduces microcracks on the BF, and the improved interfacial

bonding between the BF and epoxy resin due to the presence of KH560. When carboxylated CNTs were introduced into the composite, the flexural modulus, flexural strength and flexural strain of the BF-5%KH560-CNT/EP composite increased to 53.2 GPa, 1519.9 MPa, and 4.4% respectively, an increase of 8.8%, 20.9%, and 23.6% compared to the properties of the BF-washed/EP composite. This increase in properties is higher than the property enhancement achieved in the BF-5%KH560/EP composite and is a result of the introduction of carboxylated CNTs, which increases the infiltration of fiber and resin and the roughness of the BF surface resulting in an increase of the contact area between the epoxy resin and the BF. This enhances the mechanical meshing between fiber and resin, thus boosting the friction and interface interaction between the BF and epoxy resin matrix[8,51]. In addition, the oxygen-containing functional group/unsaturated double bond on the surface of the carboxylated CNTs can also form a solid chemical bond with the epoxy resin matrix, enhancing the interaction between the BF and epoxy resin, thus significantly improving the flexural properties of BF-5%KH560-CNT/EP[53].

As discussed in section 3.1 on surface characterization, the use of the KH560 solution at 10% mass fraction results in a degradation of the BF surface with a large amount of KH560 being physically adsorbed on the BF surface. The use of 10% KH560 also leads to large agglomerates of carboxylated CNTs being adsorbed on the BF surface, resulting in a stress concentration. Both of these phenomena reduce the flexural properties of the composite. For example, the flexural modulus, flexural strength, and flexural strain of the BF-10%KH560-CNT/EP composite were measured

to be 32.9 GPa, 1167.7 MPa, and 3.2% respectively, which is a reduction of 32.7%, 7.1%, and 9.3% respectively, compared with the BF-washed/EP composite. This decrease in flexural performance is much greater than that for the BF-10%KH560/EP composite and is caused by a local stress concentration due to CNT agglomerates [8,51,54].

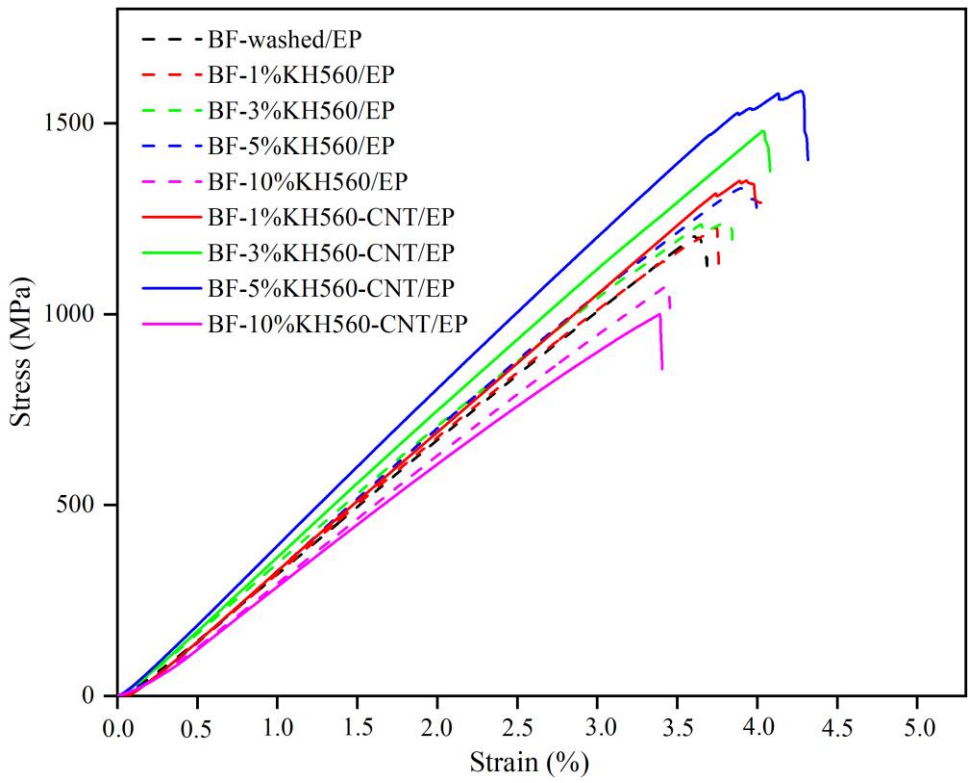

Fig. 8 Flexural stress-strain curves of BF-X%KH560/EP and BF-X%KH560-CNT/EP

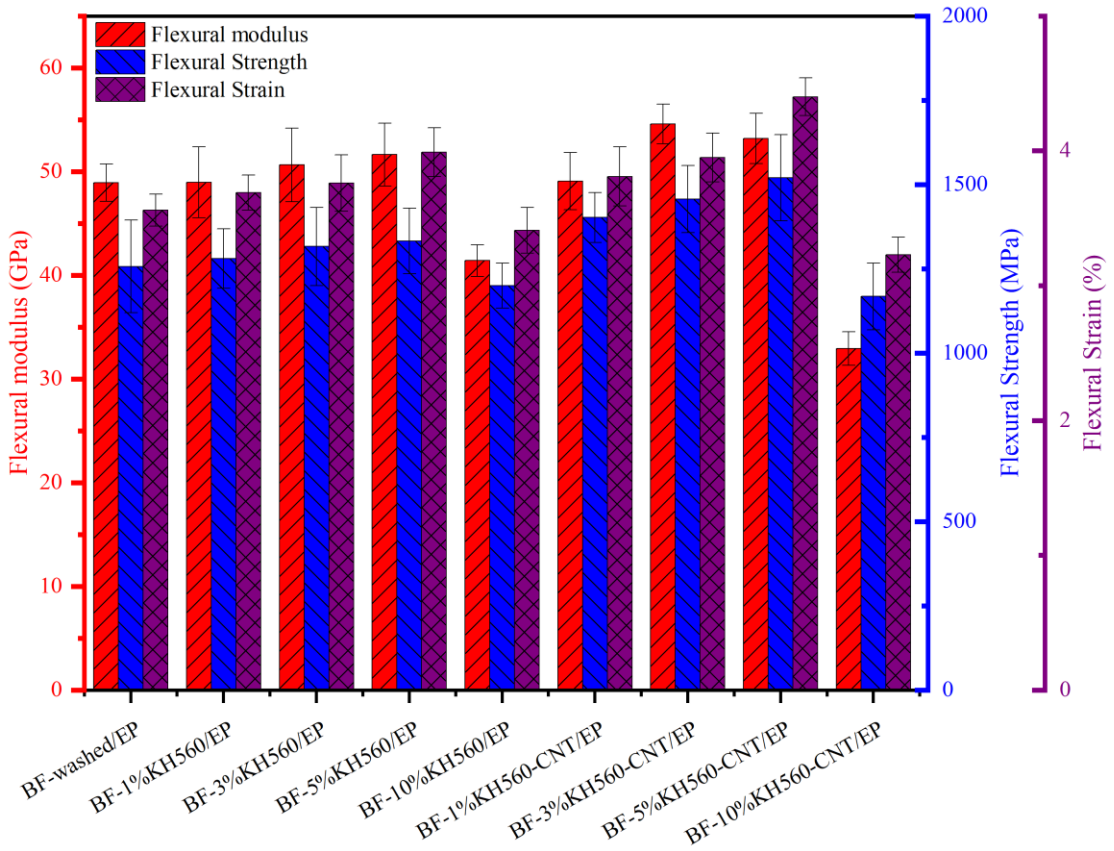

Fig. 9 Flexural modulus (E_f) and flexural strength (σ_f) and flexural strain at break (ε_f) of modified and unmodified basalt fiber reinforced resin matrix composites

Table 4 Improvement in flexural properties of BF-X%KH560/EP and BF-X%KH560-CNT/EP (standard deviations are shown in the brackets)

Sample	E_f(GPa)	ΔE_f(%)	σ_f(MPa)	$\Delta\sigma_f$(%)	ε_f(%)	$\Delta\varepsilon_f$(%)
BF-washed/EP	48.9(±1.8)	-	1256.9(±137.5)	-	3.6(±0.1)	-
BF-1%KH560/EP	49.0(±3.4)	0.2	1280.6(±88.2)	1.9	3.7(±0.1)	3.7
BF-3%KH560/EP	50.6(±3.5)	3.5	1316.2(±116.2)	4.7	3.8(±0.2)	5.6
BF-5%KH560/EP	51.6(±3.0)	5.5	1332.3(±97.3)	6.0	4.0(±0.2)	12.1
BF-10%KH560/EP	41.4(±1.5)	-15.3	1199.6(±66.9)	4.6	3.4(±0.2)	4.2
BF-1%KH560-CNT/EP	49.1(±2.8)	0.4	1402.2(±74.1)	11.6	3.8(±0.2)	7.0
BF-3%KH560-CNT/EP	54.6(±1.9)	11.7	1456.9(±99.8)	15.9	4.0(±0.2)	11.0
BF-5%KH560-CNT/EP	53.2(±2.4)	8.8	1519.9(±127.8)	20.9	4.4(±0.1)	23.6
BF-10%KH560-CNT/EP	32.9(±1.6)	-32.7	1167.7(±99.0)	7.1	3.2(±0.1)	9.3

3.2.3 Interlaminar shear strength

Fig. and Table 5 shows the results of interlaminar shear strength testing carried out following the procedure stated in section 2.4. The results show that for X⩽5, the ILSS of BF-X%KH560/EP and BF-X%KH560-CNT/EP increase to varying degrees compared with BF-washed/EP. The best properties for the BF-X%KH560/EP type composites were obtained for a 5% mass fraction of KH560. The ILSS of BF-5%KH560-CNT/EP is 105.3 MPa, an increase of 25.5%. The change in shear strength is related to the change in the failure mode of the composite interface which depends on the interface bond strength[33]. The two main failure modes of the composite are adhesion failure and cohesion failure. When the BF is not modified, the bonding force between the BF and epoxy resin is weak which results in a weak interface. In such composites, cracks propagate at the interface, and the interface failure is mainly adhesion failure. When carboxylated CNTs are introduced into the BF modified by KH560, the infiltration of fiber and epoxy resin is increased,

improving the contact between fiber and resin. This results in good wetting of the fibers and a stable interface[51]. Besides, strong chemical bonds are formed between the KH560-modified BF and the carboxylated CNTs and between the carboxylated CNTs and resin matrix to enhance the interaction between the BF and epoxy resin. Moreover, the carboxylated CNTs diffused into the matrix also form a strong interfacial bond with the matrix[33]. This strengthens and toughens the resin matrix, so that the stress can be immediately transferred from the weak matrix to the stronger CNTs embedded in the matrix. The carboxylated CNTs extending into the matrix also enhance mechanical engagement, thereby enhancing the interfacial bonding strength. All of these phenomena result in a change of the failure mode of the interface from adhesion failure to cohesion failure, which significantly improves the ILSS of the composite[53].

The results also show that when the mass fraction of KH560 is too large, the ILSS of the composite is reduced. The ILSS of BF-10%KH560-CNT/EP is 56.1 MPa which represents a decrease of 33.1% from the ILSS of the BF-washed/EP composite. This is because when the concentration of KH560 is too high, a large number of carboxylated CNTs are adsorbed on the BF surface. These CNTs are agglomerated on the fiber surface, and the dispersion uniformity is reduced, resulting in incomplete infiltration of fibers and resin, and the formation of voids and other defects in the interface area of the composite. This leads to a reduction of the interfacial bonding strength, resulting in a reduction of the ILSS of the composite.

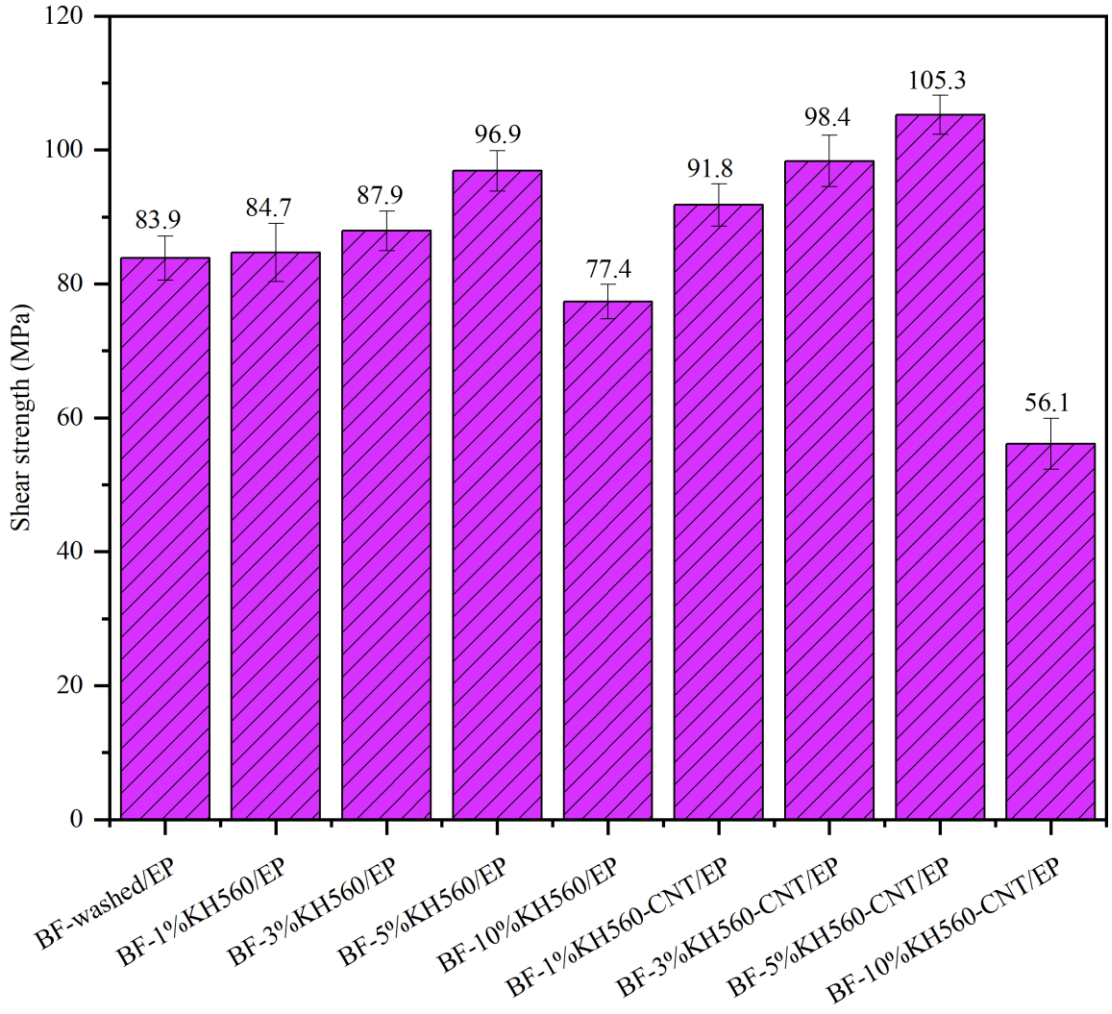

Fig. 10 ILSS of modified and unmodified basalt fiber reinforced resin matrix composites

Table 5 Improvement in ILSS of BF-X%KH560/EP and BF-X%KH560-CNT/EP (standard deviations are shown in the brackets)

Sample	ILSS(MPa)	ΔILSS(%)
BF-washed/EP	83.9(±3.3)	-
BF-1%KH560/EP	84.7(±4.4)	1.0
BF-3%KH560/EP	87.9(±2.9)	4.8
BF-5%KH560/EP	96.9(±3.0)	15.5
BF-10%KH560/EP	77.4(±2.6)	-7.7
BF-1%KH560-CNT/EP	91.8(±3.2)	9.4
BF-3%KH560-CNT/EP	98.4(±3.8)	17.3
BF-5%KH560-CNT/EP	105.3(±2.9)	25.5
BF-10%KH560-CNT/EP	56.1(±3.8)	-33.1

3.3 Fracture surface morphology of composites

SEM was used to examine the fracture surfaces of BF-washed/EP, BF-5%KH560/EP, and BF-5%KH560-CNT/EP composite samples to further investigate the modification effects of KH560 and carboxylated CNTs, as shown in Fig. 8. To gauge the quality of the interfacial bonding, the amount of resin adhering to the BF surface was observed. From Fig. 8 (a) and (a'), it can be seen that the fracture surface of BF-washed/EP composite material is flat and smooth, with only a small amount of resin adhering to the fibers. This indicates that the bonding between the BF and resin is poor. However, for BF-5%KH560/EP composite materials, a significant amount of resin was observed to adhere to BF, indicating an improvement in interfacial adhesion between BF and resin after treatment with a 5% KH560 solution, as shown in Fig. 8 (b) and (b'). In addition, after treating BF with a 5% KH560 solution and introducing carboxylated CNTs, the fracture surface of BF-5%KH560-CNT/EP was rough, and the fibers were firmly wrapped by the resin. A large amount of residual resin adhered to the exposed BF surface, and even some resin sheets adhered to BF. This indicates that the introduction of carboxylated CNTs further enhances the interfacial adhesion between BF and resin, and further improves the interfacial performance of the composite material, as shown in Fig. 8 (c) and (c'). The SEM results of the fracture surfaces of composites are agree well with the mechanical properties of composites.

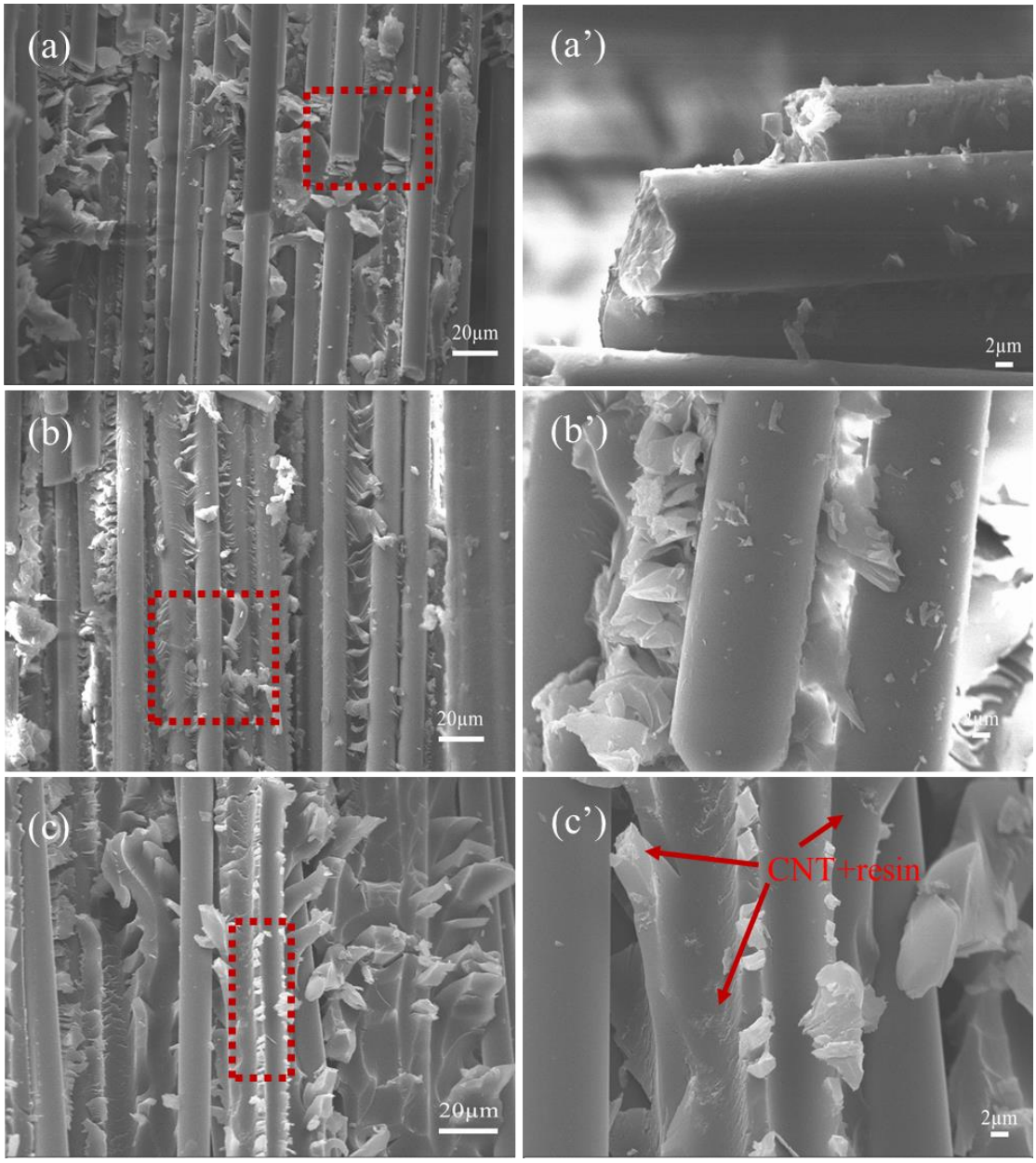

Fig. 8 SEM images of fracture surfaces of BF-X%KH560-CNT/EP: (a) and (a') BF-washed/EP, (b) and (b') BF-5%KH560/EP, (c) and (c') BF-5%KH560-CNT/EP

3.4 Thermal stability of composites

TGA was performed on BF-washed/EP, BF-5% KH560/EP and BF-5%KH560-CNT/EP composite samples.The results are shown in Fig. 9 and Table . The results show that the onset decomposition temperature of the BF-washed/EP

composite is 387 ℃, while the maximum decomposition rate temperature is 400 ℃. The onset decomposition temperature of BF-5%KH560/EP composite is 389 ℃, and the maximum decomposition rate temperature is 402 ℃. For the BF-5%KH560-CNT/EP composite, the onset decomposition temperature is 396 ℃, and the maximum rate temperature is 408 ℃. It is clear that both onset and maximum decomposition rate temperatures of BF-5%KH560/EP and BF-5%KH560-CNT/EP composite materials have been improved to a certain extent. At 800 ℃, the residual weights of BF-5%KH560/EP and BF-5%KH560-CNT/EP were slightly increased by 1.5% and 5.8% respectively compared to BF-washed/EP. Overall, the TGA results show that the thermal stability of the composites has been improved after the modification of the BF. This is because the interface property between the modified BF and the epoxy resin matrix has been improved. Moreover, the thermal properties of the composites are improved more after the introduction of carboxylated CNTs. This is because the CNTs facilitate to form a stronger interface adhesion, which has an inhibitory effect on the movement of the epoxy resin molecular chains. In addition, CNTs have a high thermal conductivity and can also promote the heat dissipation from the internal area of composite[52,55,56]

To further demonstrate the effectiveness of nanofillers in resisting thermal degradation trend, Horowitz-Metzger[57] method (Eq. 1) was used to calculate the thermal degradation activation energy:

$$ln[ln(1-\alpha)^{-1}] = \frac{E\theta}{RT_{max}^2} \quad \text{(Eq. 1)}$$

where θ is the difference between T and T_{max}, T_{max} is the temperature of

maximum rate of mass loss, and R is the gas constant, α is the conversion rate, and E is the thermal degradation activation energy.

The calculated thermal degradation activation energy of basalt fiber composite materials is listed in Table . It can be seen that the thermal degradation activation energy of the modified basalt fiber composite material is improved to varying degrees. The thermal degradation activation energy of BF-washed/EP was 269.0 kJ/mol. When carboxylated CNTs were introduced, the thermal degradation activation energy of BF-5%KH560-CNT/EP increased to 293.6 kJ/mol. This further indicates that the introduction of carboxylated CNTs increases the thermal stability of the composite material.

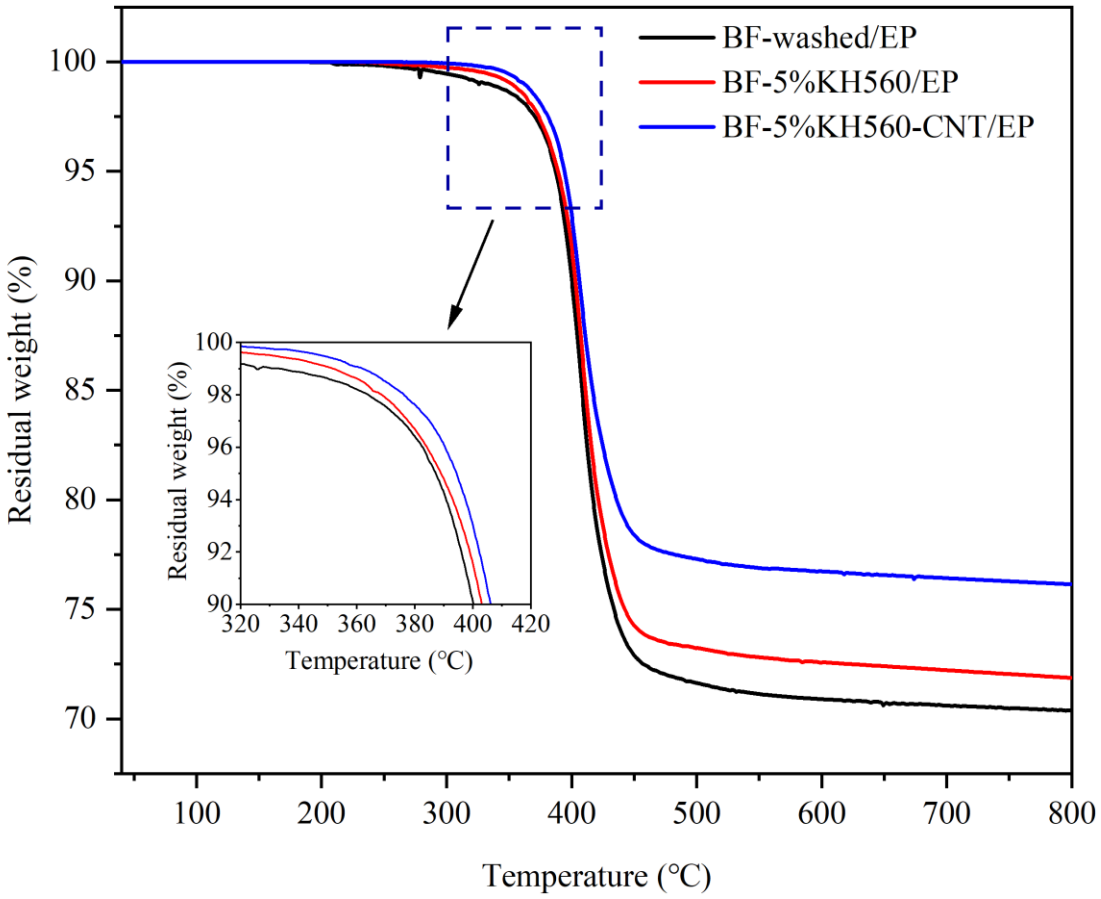

Fig. 9 TGA curves of BF-washed/EP, BF-5% KH560/EP and BF-5%KH560-CNT/EP

Table 6 TGA results of BF-washed/EP, BF-5% KH560/EP and BF-5%KH560-CNT/EP

Sample	onset decomposition temperature (°C)	maximum decomposition rate temperatures (°C)	residual mass fraction at 800 °C (%)	thermal degradation activation energy(kJ/mol)
BF-washed/EP	387	400	70.4	269.0
BF-5%KH560/EP	389	402	71.9	271.7
BF-5%KH560-CNT/EP	396	408	76.2	293.6

4. Conclusion

In this study, BF-X%KH560-CNT/EP composites were successfully prepared by

grafting carboxylated CNTs onto a BF surface using an impregnation method with silane coupling agent, KH560, acting as a bridge. The results show that the mass fraction of KH560 is a key factor for CNT adsorption on the BF surface. With an increase of the mass fraction of KH560, the mechanical properties of the BF-X% KH560-CNT /EP are enhanced. The mass fraction of KH560 for which the mechanical properties of the composite improved the most was found to be 5%. For the BF-5%KH560-CNT/EP composite, the tensile strength increased by 12.5%, the tensile modulus increased by 27.7%, the flexural strength increased by 20.9%, the flexural modulus increased by 8.8%, and the ILSS increased by 25.5% as a result of enhanced interfacial interactions. However, when the mass fraction of KH560 was increased to 10%, the mechanical properties of the composite were reduced. Surface morphology characterization showed that for this case, there were too many CNTs attached to the surface of the BF with low dispersion uniformity and high agglomeration. This resulted in incomplete infiltration of fibers and resin and an increase in local stress concentration. In addition, TGA results showed that compared with the BF-washed/EP, the onset decomposition temperature of the BF-5%KH560-CNT/EP increased from 387 ℃ to 396 ℃, the maximum rate temperature increased from 400 ℃ to 408 ℃, and the residual weight increased by 5.8%, indicating that the thermal stability of the composite was improved after BF modification.

Acknowledgements

This work was supported by the National Natural Science Foundation of China (12102374, 52173301); Sichuan Science and Technology Program (2021YFH0031, 2022JDGD0015, 2022YFH0019, 2022YFG0113); Special Funded Postdoctoral Program of Sichuan Province (0201609912); and Innovative Research Team of Southwest Petroleum University (No. 2017CXTD01).

Reference

[1] Li M, Xing D, Zheng Q-B, et al. Corrosion behaviors of basalt fiber exposed to the acids. Construction and Building Materials. 2022;1(17):316.

[2] Lopresto V, Leone C, De Iorio I. Mechanical characterisation of basalt fibre reinforced plastic. Composites Part B: Engineering. 2011;42(4):717-723.

[3] Arslan C, Dogan M. The effects of silane coupling agents on the mechanical properties of basalt fiber reinforced poly(butylene terephthalate) composites. Composites Part B: Engineering. 2018;146:145-154.

[4] Sang L, Zheng G, Hou W, et al. Crystallization and mechanical properties of basalt fiber-reinforced polypropylene composites with different elastomers. Journal of Thermal Analysis and Calorimetry. 2018;134(3):1531-1543.

[5] Uthaipan N, Jarnthong M, Peng Z, et al. Effects of cooling rates on crystallization behavior and melting characteristics of isotactic polypropylene as neat and in the TPVs EPDM/PP and EOC/PP. Polymer Testing. 2015;44:101-111.

[6] Liu J, Chen M, Yang J, et al. Study on Mechanical Properties of Basalt Fibers Superior to E-glass Fibers. Journal of Natural Fibers. 2020;19(3):882-894.

[7] Fiore V, Scalici T, Di Bella G, et al. A review on basalt fibre and its composites. Composites Part B: Engineering. 2015;74:74-94.

[8] Kim M, Lee T-W, Park S-M, et al. Structures, electrical and mechanical properties of epoxy composites reinforced with MWCNT-coated basalt fibers. Composites Part A: Applied Science and Manufacturing. 2019;123:123-131.

[9] Khandelwal S, Rhee KY. Recent advances in basalt-fiber-reinforced composites: Tailoring the fiber-matrix interface. Composites Part B: Engineering. 2020;192:108011.

[10] Preda N, Costas A, Lilli M, et al. Functionalization of basalt fibers with ZnO nanostructures by electroless deposition for improving the

interfacial adhesion of basalt fibers/epoxy resin composites. Composites Part A: Applied Science and Manufacturing. 2021;149:106488.

[11] Zhang B, Han Q, Qin H, et al. Bending resistance and anisotropy of basalt fibers laminate composite with bionic helical structure. Journal of Bionic Engineering. 2022;19(3):799-815.

[12] Jamali N, Rezvani A, Khosravi H, et al. On the mechanical behavior of basalt fiber/epoxy composites filled with silanized graphene oxide nanoplatelets. Polymer Composites. 2018;39(S4):E2472-E2482.

[13] Wang Y, Wang Y, Wan B, et al. Strain and damage self-sensing of basalt fiber reinforced polymer laminates fabricated with carbon nanofibers/epoxy composites under tension. Composites Part A: Applied Science and Manufacturing. 2018;113:40-52.

[14] Wang S, Zhong J, Gu Y, et al. Mechanical properties, flame retardancy, and thermal stability of basalt fiber reinforced polypropylene composites. Polymer Composites. 2020;41(10):4181-4191.

[15] Qian Y, Zhong J, Ou J. Superdurable fiber-reinforced composite enabled by synergistic bridging effects of MXene and carbon nanotubes. Carbon. 2022;190:104-114.

[16] Karger-Kocsis J, Mahmood H, Pegoretti A. Recent advances in fiber/matrix interphase engineering for polymer composites. Progress in Materials Science. 2015;73:1-43.

[17] Tze WTY, Gardner DJ, Tripp CP, et al. Cellulose fiber/polymer adhesion: effects of fiber/matrix interfacial chemistry on the micromechanics of the interphase. Journal of Adhesion Science and Technology. 2006;20(15):1649-1668.

[18] Lee S-O, Rhee KY, Park S-J. Influence of chemical surface treatment of basalt fibers on interlaminar shear strength and fracture toughness of epoxy-based composites. Journal of Industrial and Engineering Chemistry. 2015;32:153-156.

[19] Kim MT, Kim MH, Rhee KY, et al. Study on an oxygen plasma treatment of a basalt fiber and its effect on the interlaminar fracture property of basalt/epoxy woven composites. Composites Part B: Engineering. 2011;42(3):499-504.

[20] Li C, Wang H, Zhao X, et al. Investigation of mechanical properties for basalt fiber/epoxy resin composites modified with La. Coatings. 2021;11(6) :666.

[21] K.V B, Shirvanimoghaddam K, Rajan GS, et al. Surface treatment of Basalt fiber for use in automotive composites. Materials Today Chemistry. 2020;17:100334.

[22] Schneck TK, Brück B, Schulz M, et al. Carbon fiber surface modification for tailored fiber-matrix adhesion in the manufacture of C/C-SiC composites. Composites Part A: Applied Science and Manufacturing. 2019;120:64-72.

[23] Wen Z, Xu C, Qian X, et al. A two-step carbon fiber surface

treatment and its effect on the interfacial properties of CF/EP composites: The electrochemical oxidation followed by grafting of silane coupling agent. Applied Surface Science. 2019;486:546-554.

[24] Dighton C, Rezai A, Ogin SL, et al. Atmospheric plasma treatment of CFRP composites to enhance structural bonding investigated using surface analytical techniques. International Journal of Adhesion and Adhesives. 2019;91:142-149.

[25] Zhang C, Liu L, Xu Z, et al. Improvement for interface adhesion of epoxy/carbon fibers endowed with carbon nanotubes via microwave plasma-enhanced chemical vapor deposition. Polymer Composites. 2018;39(S2):E1262-E1268.

[26] Cech V, Knob A, Lasota T, et al. Surface modification of glass fibers by oxidized plasma coatings to improve interfacial shear strength in GF/polyester composites. Polymer Composites. 2017;40(S1) :E186-E193.

[27] Iorio M, Santarelli ML, González-Gaitano G, et al. Surface modification and characterization of basalt fibers as potential reinforcement of concretes. Applied Surface Science. 2018;427:1248-1256.

[28] Xiong S, Zhao Y, Wang Y, et al. Enhanced interfacial properties of carbon fiber/epoxy composites by coating carbon nanotubes onto carbon fiber surface by one-step dipping method. Applied Surface Science. 2021;546:149135.

[29] Yao X, Gao X, Jiang J, et al. Comparison of carbon nanotubes and graphene oxide coated carbon fiber for improving the interfacial properties of carbon fiber/epoxy composites. Composites Part B: Engineering. 2018;132:170-177.

[30] Chang C, Yue X, Hao B, et al. Direct growth of carbon nanotubes on basalt fiber for the application of electromagnetic interference shielding. Carbon. 2020;167:31-39.

[31] Khan M, Cao M, Hussain A, et al. Effect of silica-fume content on performance of $CaCO_3$ whisker and basalt fiber at matrix interface in cement-based composites. Construction and Building Materials. 2021;300:124046.

[32] Zheng Y, Sun D, Feng Q, et al. Nano-SiO_2 modified basalt fiber for enhancing mechanical properties of oil well cement. Colloids and Surfaces A: Physicochemical and Engineering Aspects. 2022;648:128900.

[33] Kuzmin KL, Timoshkin IA, Gutnikov SI, et al. Effect of silane/nano-silica on the mechanical properties of basalt fiber reinforced epoxy composites. Composite Interfaces. 2016;24(1):13-34.

[34] Hou X, Yao S, Wang Z, et al. Enhancement of the mechanical properties of polylactic acid/basalt fiber composites via in-situ assembling silica nanospheres on the interface. Journal of Materials Science & Technology. 2021;84:182-190.

[35] He H, Yang P, Duan Z, et al. Reinforcing effect of hybrid nano-coating on mechanical properties of basalt fiber/poly(lactic acid)

environmental composites. Composites Science and Technology. 2020;199:108372.

[36] Mittal G, Rhee KY. Chemical vapor deposition-based grafting of CNTs onto basalt fabric and their reinforcement in epoxy-based composites. Composites Science and Technology. 2018;165:84-94.

[37] Wu G, Ma L, Jiang H, et al. Improving the interfacial strength of silicone resin composites by chemically grafting silica nanoparticles on carbon fiber. Composites Science and Technology. 2017;153:160-167.

[38] Kurniawan D, Kim BS, Lee HY, et al. Atmospheric pressure glow discharge plasma polymerization for surface treatment on sized basalt fiber/polylactic acid composites. Composites Part B: Engineering. 2012;43(3):1010-1014.

[39] Mittal G, Rhee KY. Electrophoretic deposition of graphene on basalt fiber for composite applications. Nanotechnology Reviews. 2021;10(1):158-165.

[40] Xie Y, Hill CAS, Xiao Z, et al. Silane coupling agents used for natural fiber/polymer composites: A review. Composites Part A: Applied Science and Manufacturing. 2010;41(7):806-819.

[41] Lu Z, Kong L, He Z, et al. Modification mechanism and rheological properties of emulsified asphalt evaporative residues reinforced by coupling-modified fiber. Materials (Basel). 2021;14(23) :7363.

[42] Zhang M, Zhu H, Xi B, et al. Surface hydrophobic modification of biochar by silane coupling agent KH-570. Processes. 2022;10(301):301.

[43] Kang Y-Q, Cao M-S, Yuan J, et al. Preparation and microwave absorption properties of basalt fiber/nickel core–shell heterostructures. Journal of Alloys and Compounds. 2010;495(1):254-259.

[44] Zhang S, Zhong T, Xu Q, et al. The effects of chemical grafting 1,6-hexanediol diglycidyl ether on the interfacial adhesion between continuous basalt fibers and epoxy resin as well as the tensile strength of composites. Construction and Building Materials. 2022;323:126563.

[45] Kang Y-Q, Cao M-S, Shi X-L, et al. The enhanced dielectric from basalt fibers/nickel core-shell structures synthesized by electroless plating. Surface and Coatings Technology. 2007;201(16-17):7201-7206.

[46] Zhang X, Zhou X, Ni H, et al. Surface modification of basalt fiber with organic/inorganic composites for biofilm carrier used in wastewater treatment. ACS Sustainable Chemistry & Engineering. 2018;6(2):2596-2602.

[47] Zhai Z, He Q, Fu L, et al. Effect of plasma treatment parameters on the interfacial joining strength of overmolded hybrid fiber reinforced thermoplastic composites. Journal of Applied Polymer Science. 2022;139(20) :52166.

[48] Zhang M, Cheng C, Guo C, et al. Co-depositing bio-inspired tannic acid-aminopropyltriethoxysilane coating onto carbon fiber for excellent interfacial adhesion of epoxy composites. Composites Science and Technology. 2021;204:108639.

[49] Zhang S, Shi Z, Cui P, et al. Surface modification of aramid fibers with $CaCl_2$ treatment and secondary functionalization of silane coupling agents. Journal of Applied Polymer Science. 2020;137(39) :e49159.

[50] Sun J, Zhao F, Yao Y, et al. High efficient and continuous surface modification of carbon fibers with improved tensile strength and interfacial adhesion. Applied Surface Science. 2017;412:424-435.

[51] Liu H, Sun Y, Yu Y, et al. Effect of Nano-SiO_2 modification on mechanical and insulation properties of basalt fiber reinforced composites. Polymers (Basel). 2022;14(16):3353.

[52] Lee JH, Rhee KY, Park SJ. The tensile and thermal properties of modified CNT-reinforced basalt/epoxy composites. Materials Science and Engineering: A. 2010;527(26):6838-6843.

[53] Awan FS, Fakhar MA, Khan LA, et al. Interfacial mechanical properties of carbon nanotube-deposited carbon fiber epoxy matrix hierarchical composites. Composite Interfaces. 2018;25(8):681-699.

[54] Siddiqui NA, Li EL, Sham M-L, et al. Tensile strength of glass fibres with carbon nanotube–epoxy nanocomposite coating: Effects of CNT morphology and dispersion state. Composites Part A: Applied Science and Manufacturing. 2010;41(4):539-548.

[55] Yang W, Jia Z, Chen Y, et al. Carbon nanotube reinforced polylactide/basalt fiber composites containing aluminium hypophosphite: thermal degradation, flame retardancy and mechanical properties. RSC Advances. 2015;5(128):105869-105879.

[56] Li M, Chen Q, Li M, et al. The effect of the geometry and content of the modified carbon nanotubes on the thermal properties of the composite phase-change materials. Journal of Thermal Analysis & Calorimetry. 2021;143(1):103-112.

[57] Huang Z-G, Shi W-F. Effect of poly(bisphenol a acryloxyethyl phosphate) on the activation energy in thermal degradation of urethane acrylate. Journal of Thermal Analysis and Calorimetry. 2007;88(3):833-841.